UNIVERSIDADE FEDERAL FLUMINENSE

Incorporation of the surface dielectric function gradient and roughness effect in the model of tip-sample force in atomic force microscopy

André Gusso, gusso@metal.eeimvr.uff.br , *Universidade Federal Fluminense – PUVR/EEIMVR*

Av. dos Trabalhadores, nº420, CEP 27255-250 - Volta Redonda , RJ, Brazil

INTRODUCTION

In the last few years, several experiments based on non-contact force microscopy (nc-AFM) have been performed that revealed a strong distance dependent non-contact friction in the tip-sample interaction [Volokitin07]. A particularly relevant result was that obtained by Gotsmann and Fuchs [Gostmann01] for the dissipation between an aluminum coated silicon tip and a crystalline gold surface. They measured a strong dissipation that could be modeled as a viscous damping with a coefficient of friction varying as d^{-3}, where d denotes the tip-sample separation as measured from the contact. While this experimental result remains without satisfactory theoretical explanation, several physical models predict a non-contact friction that is a function of the tip-sample force [Volokitin07,Gusso11]. In order to discriminate the correct physical model from the experimental results for the dissipation an adequate modeling of the tip-sample force is required. So far, the long range component of the tip-sample force has been modeled simply by using the pressure predicted between two semi-spaces by the well-known Lifshitz theory [Lifshitz56] in conjunction with proximity force approximation [Hofer03]. The resulting tip-sample force has the characteristic d^{-2} dependence at short separations in the case of a spherical tip end. In order to improve the modeling of tip-sample force we include the effects of the dielectric function surface gradient and surface roughness.

Some aspects of the surface effects on the dielectric function close to the surface have recently been incorporated in the calculation of the Casimir force for the case of metals [Marusic11]. However, to the best of our knowledge, the dielectric function variation close to the surface of semiconductors and insulators has not yet been taken into account. While the changes in the electronic properties at the surface of dielectric materials has been extensively studied [Lüth10], only recently the dielectirc function was calculated as a function of the surface distance. Mendoza *et al.* [Mendoza06] calculated the linear susceptibility $X(\omega)$, which is related to the dielectric function by $\varepsilon(\omega)=1+4\pi X(\omega)$, for crystalline silicon. The results for the imaginary part of the anysotropic susceptibility for hydrogen terminated surfaces are reproduced in Fig. 1. Those results suggest that, under the simplifying assumption $\varepsilon_2(z,\omega) = \mathrm{Im}[\varepsilon(z,\omega)] = f(z)\,\varepsilon_2(\omega)$, the spatial variation in the z direction should be described by a sigmoid function.

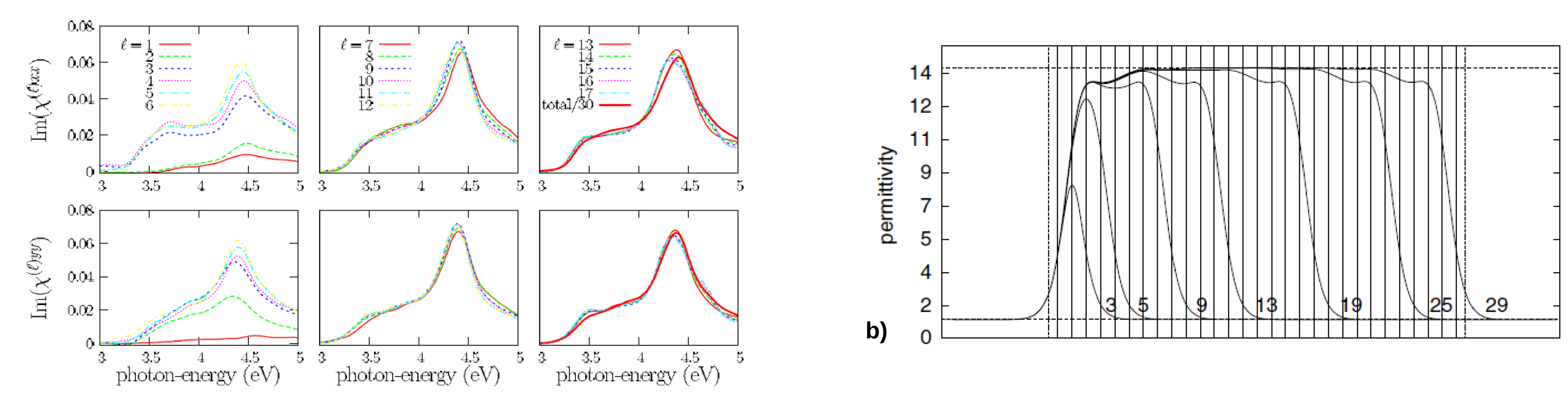

Figure 1 – a) Anysotropic linear dielectric susceptibilty for hydrogen terminated silicon surfaces [Mendoza06] and **b**) static dielectric permittivity as computed for a hydrogen terminated silicon slab [Giustino05] .

For the purpose of calculating the influence of the surface dielectric function gradient on the Casimir force we have taken $f(z)$ to vary as a quadroid function within a transition region of thickness D. The Casimir force is calculated using a multilayer approximation. Within the multilayer formalism developed by Tomas [Tomas02] and Raabe *et al.* [Raabe03] the pressure between two multilayer slabs is given by

$$P(d)=\frac{k_BT}{\pi}\sum_{n=0}^{\infty}{}'\int_0^{\infty}dqq\kappa\sum_{\sigma=s,p}\frac{r_-^{\sigma}r_+^{\sigma}e^{-2\kappa d}}{1-r_-^{\sigma}r_+^{\sigma}e^{-2\kappa d}}\ , \tag{1}$$

where $r_{\pm}^{\sigma} = r_{\pm}^{\sigma}\,(q,\xi)$ are the generalized Fresnel reflection coefficients for the s and p polarized waves reflecting from the stacks of layers above (subscript +) and below (subscript -) the gap d. In order to demonstrate the effectiveness of the multilayer approximation, in Fig. 2 we compare the predictions based on this approach with the analytical results derived by Parsegian and Weiss [Parsegian72] for the non-retarded Casimir force between two semi-spaces covered with slabs of thickness D having an exponentially varying dielectric function of the form $\varepsilon(z,i\xi)=\Gamma e^{-\lambda z}$ with ε varying between that of vaccum and bulk crystalline silicon $\varepsilon_{Si}(i\xi)$. The analytical expression for the pressure is

$$P(d)=\frac{k_BT}{8\pi d^3}\sum_{n=0}^{\infty}{}'\int_0^{\infty}\frac{x^2dx}{\left(1-e^{x}\Delta_c^{-2}\right)}\ , \tag{2}$$

where $\Delta_c = \theta(1-e^{-\beta})/[ax(1-e^{-\beta})+\beta(1+e^{-\beta})]$, $\beta=(\theta^2+a^2x^2)^{1/2}$, $\theta=\lambda D=-\ln[\varepsilon_{Si}(i\xi)]$, and $a=D/d$. It can be seen in Fig. 2a) that the prediction based on the multilayer approach in the non-retarded regime, obtained by taking the limit $c\to\infty$, coincides with the result obtained from Eq. (2) for the non-retarded Casimir force. For the sake of further comparison, the force for sharp boundaries is also shown in Fig. 2a) which results to be larger than that for the case with a surface dielectric function gradient. At this point, it is worth to note that a general consequence of the presence of surface layers having $\varepsilon_2(z,\omega)$ with values varying between those of the gap dielectric function and those of the bulk is not only to decrease the force compared to those for sharp boundaries, but also to change the dependence of the Casimir force on the gap d. Due to the relevance of a precise knowledge of the dependence of the Casimir force on the tip-sample separation for the interpretation of nc-AFM measurements we have also analyzed how the expected dependence of the force on the separation d, of the form $P(d)\sim d^{-\alpha}$, changes as a function of the surface separation. For this purpose it is useful to calculate the effective, or local, exponent α which is calculated as $\alpha = -d\,\partial\ln[P(d)]/\partial d$. The resulting exponent is presented in Fig. 2b). It can be seen that the exponent departs quite significantly from the expected value of $\alpha\approx 3$. The general trend is the exponent to decrease for shorter separations, indicating a slower rate of change of the force, the decrease being larger the larger the thickness of the region with varying ε.

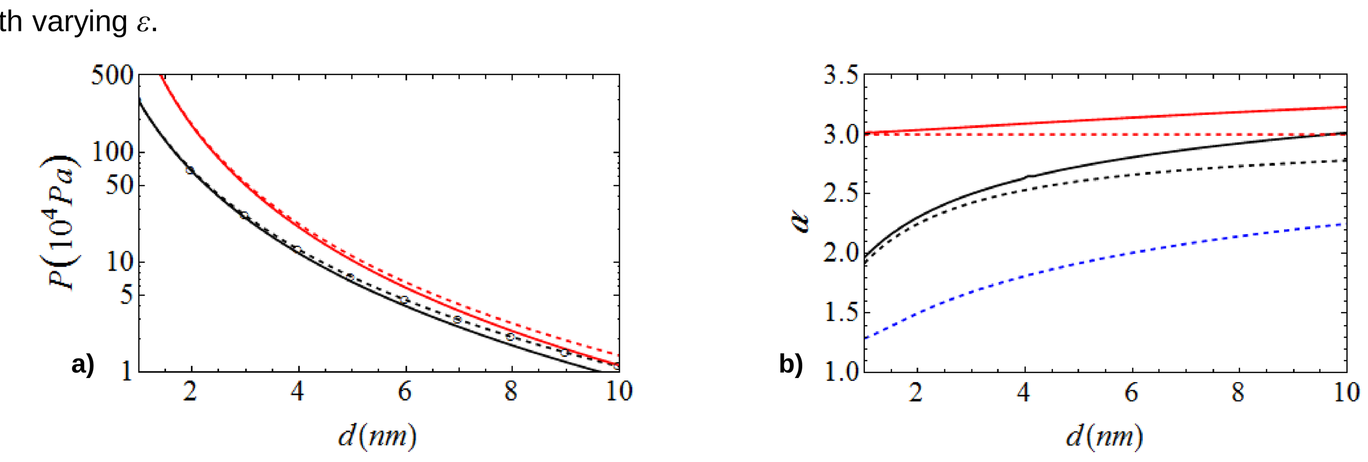

Figure 2 – a) Pressure between two crystalline silicon semi-spaces with sharp boundaries (red curves), and covered with a 1 nm thick layer with exponentially varying dielectric function (black curves). Dashed curves represent analytical results with retardation disregarded, and the continuous curves the results using the full Lifshitz theory (red) and a multilayer approach with 7 sublayers (black). The circles are the results for the multilayer approach taking the limit of an infinity speed of light. **b)** black and red curves present the corresponding effective exponent for the same cases depicted in **a)**. The blue line corresponds to the exponent for the force predicted by the analytical expression in the case of a transition region with thickness D = 5 nm.

MODEL AND RESULTS

For the particular case of crystalline silicon surfaces, the results of Mendoza *et al*. [Mendoza06] suggest that the trasition of the values of $\varepsilon_2(z,\omega)$ from those of the vaccum to those of the bulk silicon takes place over a region with thickness D of approximately 0.7 nm. For this reason we assume this value for the thickness of the region over which $\varepsilon_2(z,\omega)$ varies following a quadroid function. In order to clarify the consequences of the smooth variation of ε_2 on the Casimir force, in Fig. 3a) the resulting pressure calculated using the multilayer approach (with 7 sublayers at each surface) is compared with the pressure for sharp boundaries. In the range of distances going from 1 nm up to 25 nm, the correction to the force is of at least about -5%, reaching a quite significant maximum value of -65%. This correction can be compared with the estimated effect of spatial dispersion (nonlocality), which amounts to approximately -10% for d ~ 1 nm for both graphite [Li05] and gold [Sirvent12], decreasing rapidly with increasing d. It is worth to note that even if a sharper transition region is assumed its effect on the force remains quite significant, as can be inferred from the results presented in Fig. 3a) for D of 0.5 and 0.6 nm. As expected, the dielectric function surface gradient results in a smaller effective exponent as can be seen in Fig. 3b).

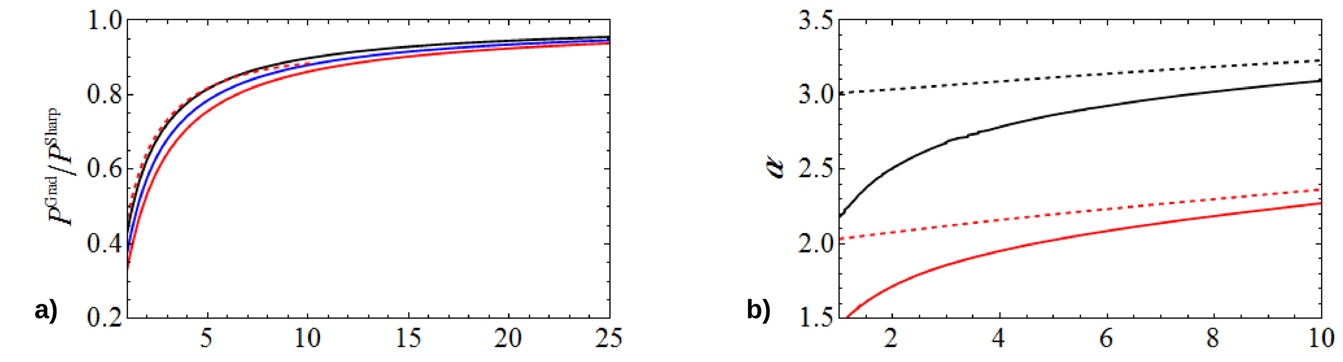

Figure 3 – a) The ratio between the Casimir force with a dielectric function surface gradient P^{Grad} and sharp boundaries P^{Sharp}. The curves are for D = 0.5 nm (black), 0.6 nm (blue), and 0.7 nm (red). The red dashed line is the ratio for the tip-sample force for D = 0.7 nm. **b)** Effective exponent for the Casimir force between two silicon semi-spaces with sharp (black/dotted) and smooth (quadroid) boundaries (black/full) and for the tip-sample force with sharp (red/dotted) and smooth boundaries (red/full).

We have also calculated the sole effect of the dielectric function surface gradient on the tip-sample force. For that purpose, the force is calculated using the proximity force approximation applied to the interaction between a sphere (spherical tip approximation) and a plane surface. The tip-sample force is calculated from the force between two plane parallel surfaces $P(d)$ as

$$F(d)=2\pi R\int_d^{\infty}P(l)dl\ , \tag{3}$$

where d denotes the closest tip sample-separation. In Fig. 3a) the resulting effect on the tip-sample force is presented as the red dashed line. While the ratio P^{Grad}/P^{Sharp},according to Eq. (3), is independent of the tip radius R, the validity of the calculated forces depends on R and d. As a consequence, for the assumed value of R = 100 nm, the calculations are limited to $d\le R/10$ = 10 nm. The resulting effective exponent is presented in Fig. 3b).

As exemplified by the images presented in Fig 4a) and 4b), an AFM tip is generally comprised of a rough surface. Futhermore, due to the small scales involved, strong non-equilibrium processes tend to favour the formation of surfaces having short scale roughness. That means that at the tip surface the correlation length λ is of the order of the rms roughness σ. If that is the case, the contribution of the surface roughness to the Casimir force can be calculated using the multilayer effective medium model (MEMM) [Gusso12]. As in [Gusso12], here we assume a rough surface having a Gaussian heigth distribution. In this ongoing work the final goal is to calculate the tip-sample force between a rough tip and an atomically flat surface including simultaneously the effects of the surface roughness at the tip and the dielectric function surface gradient at both tip and sample. For that purpose the effective dielectric function at the rough surface should be calculated using the Bruggeman mixing rule [Bruggeman35] generalized in order to account for the contribution of the layer with spatially varying dielectric function. This approach can be better understood through Fig. 4b) where an schematic diagram depicts the model tip-sample system. However, so far, in our calculations we have included the effects of the dielectric function surface gradient at the bottom surface and at the tip (or top surface) only the roughness is considered. More specifically the effective dielectric function ε^{eff} is given simply by the two component Bruggeman mixing rule

$$(1-\gamma)\frac{1-\varepsilon^{eff}}{1+2\varepsilon^{eff}}+\gamma\frac{\varepsilon_{Si}-\varepsilon^{eff}}{\varepsilon_{Si}+2\varepsilon^{eff}}=0 \tag{4}$$

where ε_{Si} denotes the complex dielectric function of bulk silicon and γ the volume fraction of silicon. In our calculations the transition region at the flat surface was modeled as described previously, by a quadroid function. In its turn, the rough surface was modeled by 7 sublayers with thickness of 0.4σ. Having the rough surface mean as a reference, we have considered 4 sublayers extending up to 1.6σ out of the surface, and 3 sublayers in the opposite direction as depicted in Fig. 4d). In the calculations we have taken σ = 1 nm, a value typically found for comercial AFM tips [Liu07] and a mean tip radius of 100 nm.

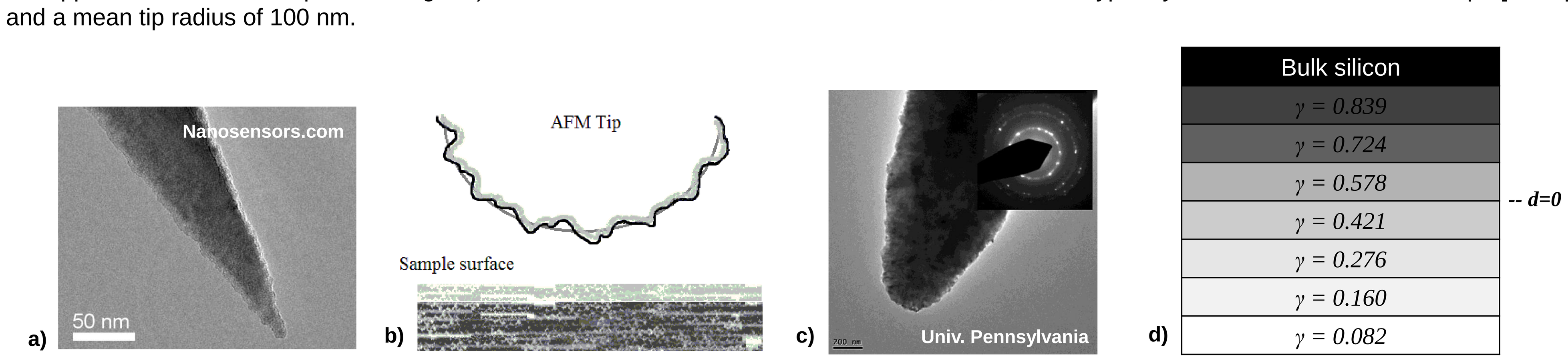

Figure 4 – SEM image of **a)** silicon and **c)** diamond AFM tips. **b)** Schematics of rough tip on top of an atomically flat sample surface. **d)** Roughness surface profile used for the calculations using the MEMM.

In Fig. 5a) the Casimir force calculated including the combined effect of the dielectric function surface gradient and surface roughness is compared with the prediction for sharp boundaries. When the distance d is measured from the mean surface distance, a convenient choice for the presentation of theoretical results, the effect of surface roughness is to increase the Casimir force. We note that in this case, if l denotes the separation between the stack of layers (the gap denoted by d in Eq. (1)), the mean separation is given by $d = l + 1.6\sigma$. In its turn, in AFM measurements its is generally the case that the only experimentally accessible distance is that whose reference (d' = 0) is taken at the point of contact. These two distance scales are usually shifted by a distance of the order of a few σ, that means $d = d' + \alpha\sigma$. Due to its relevance for the interpetration of experimental results and further comparison with theoretical predictions in Fig. 5a) we also present the pressure/force ratio when the distance is measured with distinct mean separation upon contact. In this case, the resulting force is significantly smaller than the one for sharp boundaries.

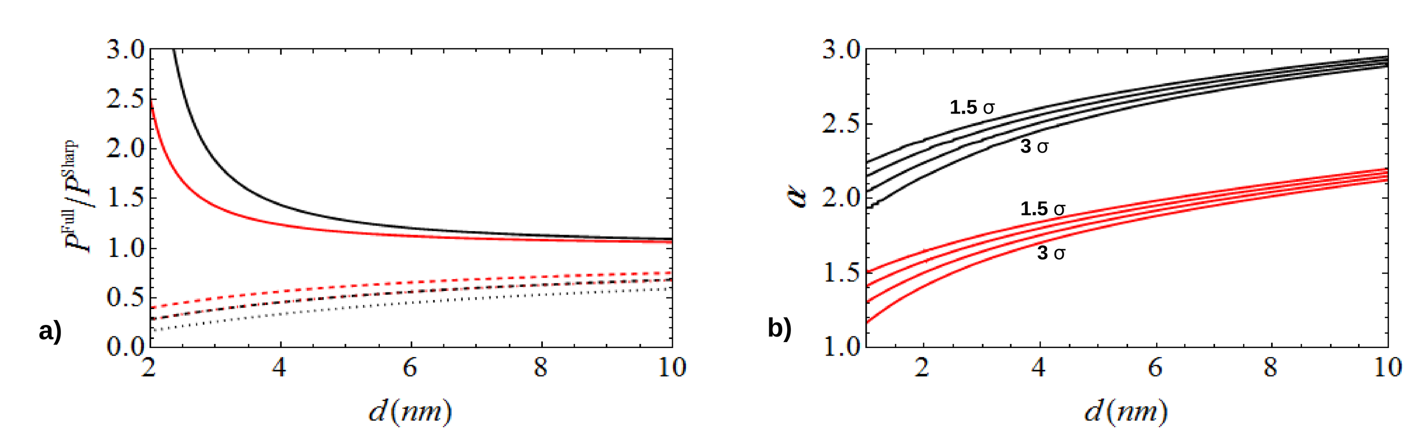

Figure 5 – a) The ratio between P^{full}, the pressure/force calculated considering the dielectric function surface gradient at the bottom surface and the roughness at the top surface/tip and P^{Sharp}, for sharp boundaries. Black curves correspond to the pressure between flat surfaces and the red curves to the tip-sample force. The distance d corresponds to the mean surface separation (full), contact at 1.5σ (dashed) and 2σ (dotted). **b)** Effetive exponent for the pressure between two flat surfaces (black) and the tip-sample force (red) including the dielectric function surface gradient at the bottom surface and the roughness at the top surface/tip. The effective exponent when the contact takes place at 1.5σ, 2σ, 2.5σ, and 3σ from the mean surface/tip-sample separation (d = 0 would correspond to contact between a top surface asperity and the flat bottom surface).

To conclude, in Fig. 5b) we present the effective exponent for the cases of interest in AFM measurements. Because the actual mean separation at contact can vary depending on the actual surface profile, we present the results for a mean separation upon contact varying from 1.5σ up to 3σ. The strong influence of both the dielectric function surface gradient and roughness correction on the effective exponent is quite evident. For the tip-sample interaction the exponent is considerably smaller than the value α = 2 usually expected at short separations. We can advance, on the basis of the results obtained so far, that the inclusion of the dielectric function gradient at the tip will result in further decrease of both the magnitude and the rate of change (and consequently the effective exponent) of the tip-sample force. Therefore the interpretation of experimental data depending on the tip-sample force can change significantly under a more reallistic modiling of this force as we are considering in this work.

ACKNOWLEDGEMENTS

The author acknowledges the financial support from Fundação Carlos Chagas Filho de Amparo à Pesquisa do Estado do Rio de Janeiro - FAPERJ, Conselho Nacional de Desenvolvimento Científico e Tecnológico - CNPQ , Fundação Euclides da Cunha (FEC-UFF) and PASI

REFERENCES

[Bruggeman35] D. A. G. Bruggeman, Ann. Phys. 24, 636 (1935).
[Giustino05] F. Giustiuno, *Infrared properties of the Si-SiO$_2$ interface from first principles*, PhD Thesis (2005).
[Gusso11] A. Gusso, J. Appl. Phys. 110, 064512 (2011).
[Gusso12] A. Gusso and U. B. Reis, EPL 99, 36003 (2012).
[Li05] Je-Luen Li *et al*., Phys. Rev. B 71, 235412 (2005).
Lifshitz56] E. M. Lifshitz, Sov. Phys. JETP 2, 73 (1956) .
[Liu07] D.-L. Liu, J. Martin, and N. A. Burnham. Appl. Phys. Lett. 91, 043107 (2007).
[Lüth10] H. Lüth, *Solid Surfaces, Interfaces and Thin Films* (Springer, 2010).
[Marusic11] L. Marušić, Vito Despoja and Marijan Šunjić, Solid State Communications 151, 1363 (2011).
[Mendoza06] B. S. Mendoza, F. Nastos, N. Arzate and J. E. Sipe, Phys. Rev. B 74, 075318 (2006).
[Parsegian72] V. A. Parsegian and G. H. Weiss, J. Colloid Interface Sci. 40, 35 (1972).
[Raabe03] C. Raabe, L. Knöll, and D.-G. Welsch, Phys. Rev. A 68, 033810 (2003).
[Sirvent12] E. Esquivel-Sirvent and G. C. Schatz, J. Phys. Chem. C 116, 420 (2012).
[Tomas02] M. S. Tomas, Phys. Rev. A 66, 052103 (2002).